# Quantifying Crop Water Consumption and Stress Patterns in Bagpath District, Western Uttar Pradesh: A Comprehensive Analysis Using Multidate Resourcesat Satellite Data

**[1] Dr. V.Charan Kumar Reddy, [2] M. Reddi Bhaskara Reddy (Associate Professor), [3] Paavan Kumar Reddy Gollapalli.**

**[1&2] Department of Geography, Sri Venkateswara University, Tirupati, Andhra Pradesh India.**
**[3] Secretary, WG-SDTA, International Commission on Irrigation and Drainage**

## Abstract

This research utilizes remote sensing techniques and incorporates NDVI-based classification methods to estimate crop evapotranspiration (ETc) in the region of Bagpath, located in Western Uttar Pradesh. The approach employs NDVI profiles to accurately map sugarcane-wheat and rice-wheat cropping systems, achieving an accuracy of 86.86% for Kharif crops and 79.72% for Rabi crops. The potential evapotranspiration exhibits seasonal variations, characterized by significant peaks in Kcb values between the months of September and February for both systems. The research examines the variation in ETc, ranging from 3.09 to 6.87 mm day−1, throughout the period of June 2017 to April 2018, with a specific focus on the water requirements for cultivating sugarcane. The dynamics of water stress, as shown by WS_LSWI data, exhibit a correlation with the various phases of crop development, therefore emphasizing the influence of harvesting operations on the levels of water stress.

## 1. Introduction

Agriculture has significant importance across all economic sectors due to its susceptibility to water constraint. At present, the agricultural sector is responsible for around 70% of the total worldwide freshwater withdrawals. Water has a pivotal role as an essential element in the process of food production. Given the substantial water transpiration demands associated with biomass production, it would not be inaccurate to assert that agriculture serves as both a catalyst and a casualty of water shortage. The exponential increase in population has resulted in significant environmental consequences due to the escalating demands placed on natural resources. The potential effects of climate change on water supplies and water demand, as well as the influence of bioenergy generation on agriculture, are subjects that now lack certainty. Climate change has the potential to modify hydrological patterns and the accessibility of freshwater resources, hence affecting both rain-fed and irrigated agricultural practices (FAO, 2008; FAO, 2011a). There has been seen an augmentation in precipitation levels within temperate regions, along by a decline in precipitation within semi-arid areas. Additionally, there has been noted a heightened variability in the distribution of rainfall, coupled with an overall rise in temperature. The aforementioned factors have a distinct influence on agriculture in tropical and sub-tropical regions. Changes in runoff in rivers and recharging of aquifers have a significant impact on the availability of water, hence exacerbating the strain on water resources caused by human activities.

India has a significant scarcity of water resources, as it accommodates around 16.0 percent of the global population but possesses just 4.0 percent of the available fresh water suitable for use. The irrigation industry is the largest consumer of water resources. Approximately 80% of the global water resources are allocated for the purpose of irrigation. In India, irrigation accounts for almost 80% of the used water resources. The projected water resources of India amount to 4000 cubic kilometers, based on the country's geographical

size of 3.3 million square kilometers and an average annual rainfall of 1170 mm. Approximately half of the water undergoes various processes such as evaporation, percolation, and subterranean flows towards the seas, resulting in a loss. Consequently, only a total of 1953 Billion Cubic Meters (BCM) of water is accessible. According to Phansalker and Verma (2005), the presence of water is subject to temporal and spatial fluctuations, resulting in a further reduction to 1086 BCM. According to estimates, the Annual Water Resource, which measured 2214 cubic meters in 1996, is projected to decrease to 1496 cubic meters by the year 2025. According to Gulati et al. (2005), the Developed Water Resource (DWR) accounts for about 25% of the total accessible water resource.

Low water availability limits plants. Stomata regulate plant water, oxygen, and carbon dioxide flow. Water stress causes stomata to shut to save water, limiting the oxygen, water, and carbon dioxide exchange route and decreasing photosynthesis (Porporato et al., 2001). Thus, water stress affects leaf development more than root growth because roots can adjust. Reduced photosynthesis due to water scarcity reduces crop growth and development. Soil moisture, canopy temperature/evapotranspiration (ET), leaf water content, and LWP affect crop water stress.

Water stress detection helps farmers reduce output losses. Remote sensing and ground-based methods may identify water stress.

Traditional stress assessment methods include predawn leaf water potential (Dixon, 1914), leaf pigment concentration (Lichtenthaler, 1987), leaf chlorophyll fluorescence (Muller, 1874) and ET (Priestley and Taylor, 1972). Predawn leaf water potential estimation employs pressure chamber. This method has measured tree and shrub water relations for 40 years. Manual operation is sluggish and laborious. Leaf water content approach analyzes plant water status by measuring relative leaf water content. Most plant water is in mesophyll cells. The ratio of fresh, dry, and turgid leaf weights determines relative leaf water content. This approach is time-consuming since the water potential difference between stressed and non-stressed plants is largest in the morning. Leaf pigment concentration approach assumes plant pigment concentration changes with species, phenology, and natural and human stress. Chlorophyll levels are higher in healthy plants and lower in stressed ones. Traditional chemical methods involve destructive sample and time-consuming laboratory studies, whereas chlorophyll meters are simple, portable, and fast. Leaf chlorophyll fluorescence is being employed to study photosynthetic equipment. This approach employs a portable optical equipment and fluorescence meter. Photosynthesis is dependent on light, water, and nutrients, which cause plant stress. Thus, this device is a useful diagnostic of plant stress because Chlorophyll fluorescence changes before tissue degradation is noticed in plants, allowing stress to be diagnosed before physical damage. The downside is that this method does not produce commercial instruments. Plant ET is measured with lysimeters.

All ground-based measurements can quantify plant water stress at ground level or local regional level, but not at large geographical scales like remote sensing. Either ground measurement can ground truth remote sensing applications.

Remote sensing for plant and environmental research became popular in the 1980s.Remote sensing provides accurate, quantitative, and timely crop condition data at a lower cost than field approaches (Shen et al., 2009). Remote sensing detects crop growth, stress, and assists agricultural development decisions (Shen et al., 2009). The spectral characteristics of vegetation are determined by leaf internal structure and elements like water, nitrogen, cellulose, and lignin absorption and scattering. Leaves' cellular structure and water content are identified in near and mid-infrared, while their colors are recognized in visible band.

Chlorophyll and water content are key plant stress indicators. Stressed flora has less chlorophyll, which affects leaf pigment light absorption. Therefore, it directly impacts plant spectral signature by lowering

green band reflection and increasing blue and red band reflection, modifying normal plant spectral signature. Thus, Visible, Near Infrared (NIR), SWIR, and TIR bands may detect water stress. Vegetation water stress index (VWSI) and Land Surface Wetness Index (LSWI) are SWIR and NIR indices (Ghulam et al., 2007), while Crop Water Stress Index (CWSI) and Water Stress Index (WSI) are TIR indices.

Precision agriculture depends on irrigation scheduling to avoid water stress and maximize production under restricted water circumstances, hence satellite monitoring of vegetation water stress is crucial. This research used optical data to diagnose sugarcane water stress in Bagpath, western UP.

## 2. Study Area

The study area includes Bagpath, located in Western Uttar Pradesh. The Western U.P region makes a significant contribution to the overall food grain output, accounting for 34 percent at the state level and 6 percent at the national level. The prevailing agricultural produce in this area is sugarcane.

The research region is situated within the latitudinal range of 28.8 degrees to 29 degrees and the longitudinal range of 77 degrees to 77.5 degrees. The western region is geographically demarcated by the presence of the Yamuna River, which serves as a natural boundary separating it from the neighboring states of Haryana and Delhi. The research was carried out in the Bagpath district located in western Uttar Pradesh.

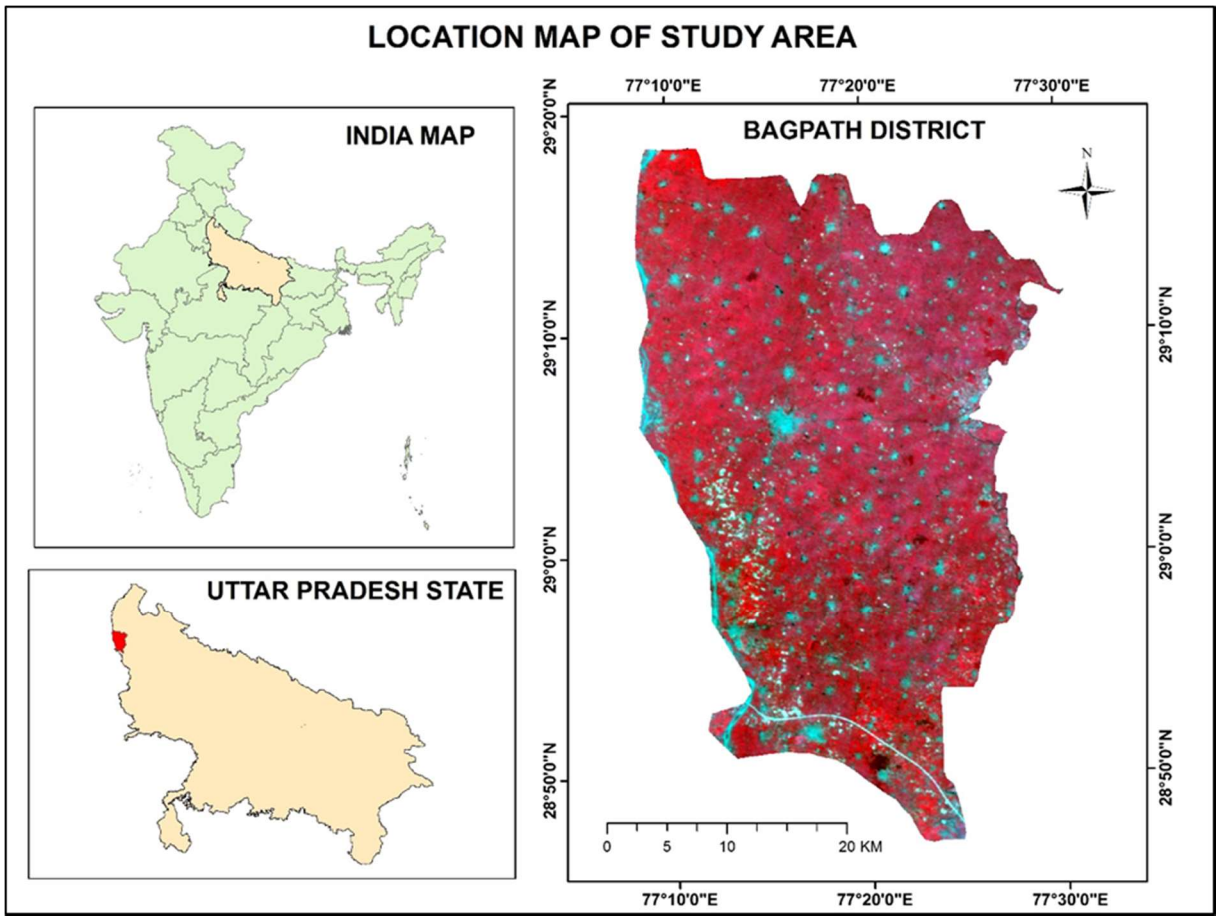


**Fig 1. Location Map of the study area**

### 2.1 Soils

Western UP soil is coarse-to-medium alluvium and somewhat alkaline. Their dark gray color indicates considerable organic matter. Loam and silty clay loam cover much of the terrain. 2016 (Nitika et al.)

### 2.2 Farming Method

Farmers' main business is crop production. This area also farms dairy. Agro-horticulture and agro-forestry are other growing agricultural industries in this area. Sugarcane dominates this region's commercial crop. Due to delayed sugarcane harvesting, wheat field preparation begins in November and lasts until the second week of December. Over 90% of land is irrigated wheat, which receives 4–5 irrigations. 2016 (Nitika et al.)

## 3. Materials and Methodology

Evapotranspiration of crops ETc provides the foundation for agricultural water needs assessment and irrigation control. This study evaluated ETc using satellite-derived ETo and Kcb. ETc was calculated for the whole research region after satellite image preprocessing. ETo is most often calculated using the FAO-56 technique, which is retrieved daily from MOSDAC. NDVI is used to determine the basal crop coefficient Kcb, as detailed below.

### 3.1 Data Used

Satellite products, supplementary data, and software were employed to fulfill the study's goal.

### 3.2 Remote sensing data

Table 3.2 lists the satellite dataset utilized in this investigation.1. AWIFS data was unavailable in February, March, and April 2018, hence Sentinel data was utilized.

| S. No | Data Type | Date of Acquisition | Resolution |
|---|---|---|---|
| 1 | Sentinel-2A | 25th April 2018<br>26th March 2018<br>14th February2018 | 10 m (Resampled to 56 m) |
| 2 | AWiFS | 4thJune 2017<br>27th September 2017<br>17th October 2017<br>20th November 2017<br>18th December 2017 | 56 m |

| | | | |
|---|---|---|---|
| | | 30th January 2018 | |
| 3 | INSAT-3D (PET_Daily) | 8th April 2017<br>11th May 2017<br>4th June 2017<br>27th September 2017<br>17th October 2017<br>20th November 2017<br>18th December 2017<br>30th January 2018 | 5 km (Resampled to 56 m) |
| 4 | MOD04, 05, 08 Products | For Aerosal Optical Depth, Water Vapour and Ozone | Source Giovanni(Average value data) |

**Table 3.2 Details of satellite data products used in this Study**

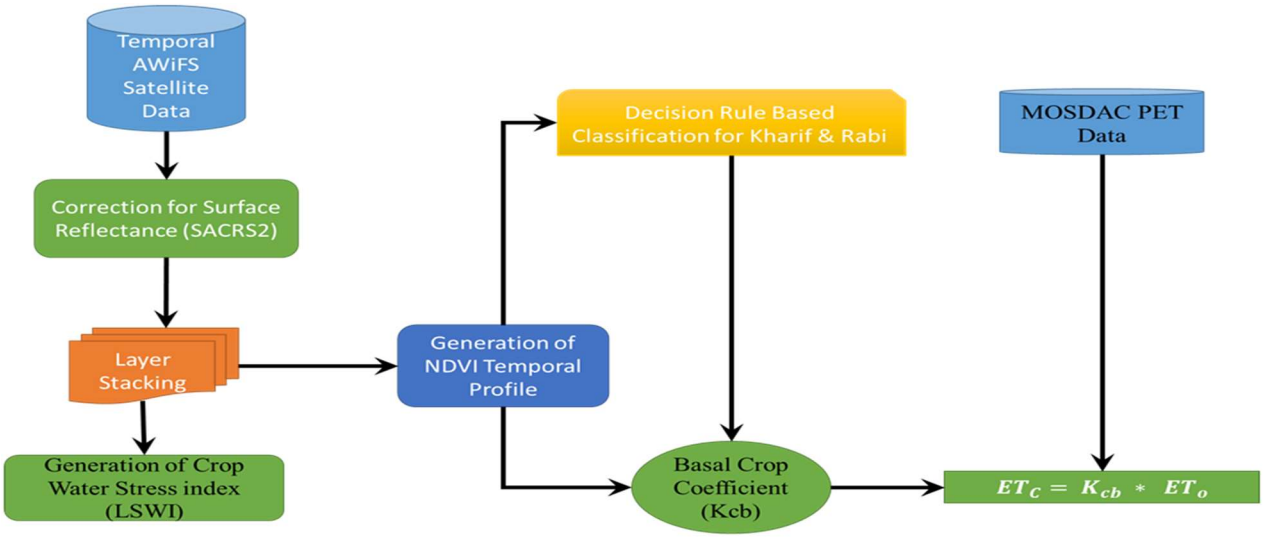


**Fig 2. Methodology flowchart**

### 3.3 Basal Crop Efficient

Estimating crop ETc for irrigation scheduling using crop coefficient methods is common. Generalized crop coefficient curves in the literature only estimate ETc for "optimum" crop conditions within a field, which must be modified for local conditions and cultural practices and adjusted for seasonal crop and weather variations. Thus, generalized crop coefficient uncertainties may lead to ETc predictions that are considerably different from real ETc, which might lead to poor irrigation water management. Crop attributes like percent cover and leaf area index may be modeled using vegetation indices (VIs) to quantify real-time crop fluctuations from remotely-sensed VI measurements. VIs can also predict the basal crop coefficient (Kcb) for maize and cotton, according to limited studies. This study estimated Kcb using NDVI measurements.

$$\boldsymbol{K_{cb}} = \boldsymbol{K_{cb\,max}} \frac{(\boldsymbol{NDVI - NDVI_{min}})}{(\boldsymbol{NDVI_{max} - NDVI_{min}})} \qquad (1)$$

Where $\boldsymbol{K_{cb\,max}}$ is Basal crop coefficient and $\boldsymbol{K_{cb\,max}}$ is Basal crop coefficient at effective full ground cover i.e., (Hunsaker, 1994)

### 3.4 Evapotranspiration potential

INSAT 3D is a geostationary meteorological satellite launched in 2013 as an exclusive INSAT spacecraft. This radiometer has four bands: wide VIS (0.52-0.75), SWIR (1.55-1.70), MIR (3.8-4.0), WV (6.5-7.0), and thermal TIR1(10.2-11.2), TIR2 (11.5-12.5) with 19 sounder channels. VIS and SWIR have 1 km x 1 km spatial resolution, whereas MIR, WV, and two thermal IR bands have 4 km x 4 km. INSAT Meteorological Data Processing System (IMDPS) automates ‘full-globe’ and ‘sector’ data products in all bands at half-hour intervals at 4 km spatial resolution. Daily purchases are limited to 48.

Evapotranspiration (ET) drives the hydrological cycle. ET is unique in its position as a link between the energy and water cycles. Solar radiation, wind speed, air temperature, and vapour pressure deficit affect ETo. Solar radiation is the most sensitive, affecting ETo variability by 60-70%. PET, also known as grass reference ETo, is the quantity of water transferred per unit time to atmosphere from a water-non-limiting surface covered with evenly and actively growing short grass like Alfalfa. ETo is the atmospheric evaporative demand for a given climate. Water stress results from moisture deficiency. Reference Evapo-transpiration is a hydrological and agricultural variable. It is a crucial input in soil water balance models together with precipitation. Many of these models use daily or hourly evapotranspiration data to predict plant water needs. The regional water demand would vary by agroclimatic conditions and agricultural season. Space rainfall and ETo may enable rainfed agriculture monitor water shortfall and excess throughout growing season. PET product accuracy is 80-90% (INSAT-3D Manual, 2015).

### 3.5 Crop Evaporation Transmission

Crop ETc is the evapotranspiration of a disease-free crop produced in wide fields with plenty of water and fertilizer (Doorenbos and Pruitt, 1977). Calculating soil water balance and irrigation schedule requires ETc estimation. Weather and crop conditions determine ETc. ETc is mathematically represented as $\boldsymbol{ET_C = K_C * ET_O}$ (2)

Kc is the crop coefficient, which varies by crop and growth stage, and ETo is the reference crop evapotranspiration.

### 3.6 Land Surface Wetness Index

LSWI assesses stress using NIR and SWIR. This measure is sensitive to soil background and total vegetation liquid. LSWI was estimated using this equation:

LSWI=NIR-SWIR/NIR+SWIR (3)

Water stress scalar (Ws) was calculated using estimated LSWI (Xiao et al., 2005).

$$W_S = \frac{1-LSWI}{1+LSWI_{max}} \quad (4)$$

Where LSWI is pixel value and LSWImax is maximum pixel LSWI value for growth season.

## 4. Results and Discussion

### 4.1 Crop discrimination

Each crop has a distinct spectral signature, therefore remotely sensed data can distinguish crops. Typical crop spectral reflectance displays pigment absorption in visible area (0.62-0.68 m) and significant near infrared reflection owing to leaf cellular structure. Red absorption and near-infrared reflectance indicate crop health (Navalgund et al., 1991b).

A rule-based classification analysis identified and distinguished rice, sugarcane, and wheat crops from other land use/land cover groupings. Rule-based feature selection using basic mathematical logics is successful. For crop discrimination, AWiFS temporal NDVI was utilized to create rules based on NDVI values of

various seasons, such as September. The transformation NDVI*127.5+127.5 linearized NDVI values between 0-255 (Ray S S et al., 2000).

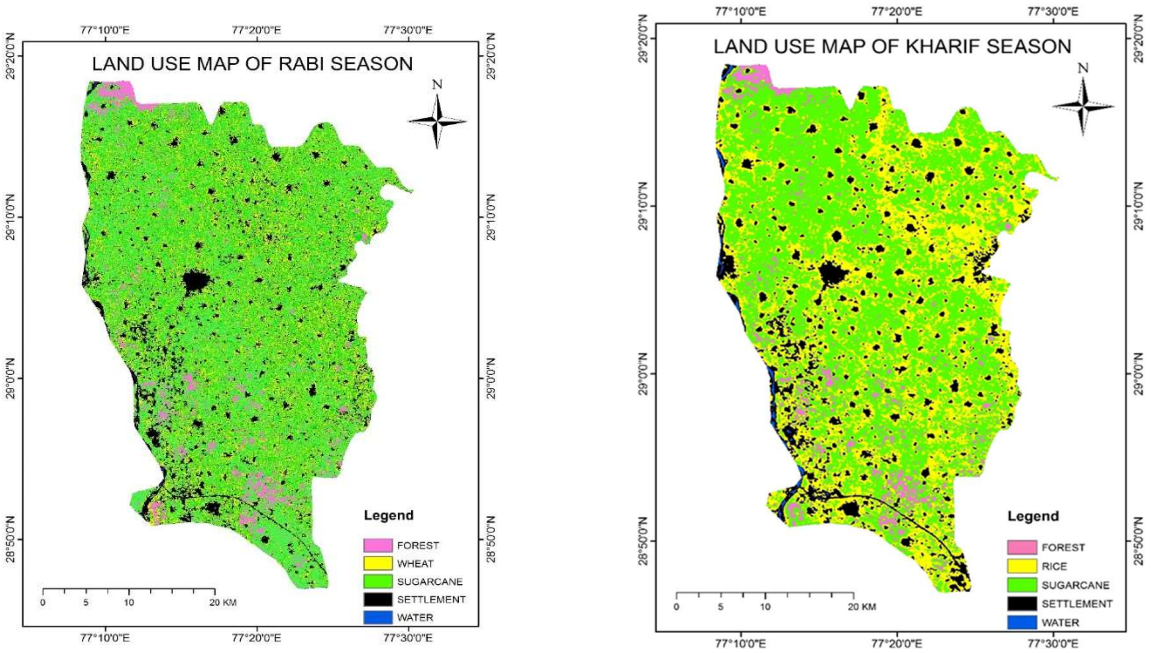


**Fig 3. Shows the crop inventory map of Kharif Season & Rabi Season**

### 4.2 NDVI Variation Throughout the Crop Season

A time-series of NDVI was created from all 9 AWiFS dates throughout crop growing seasons. Figure 4 show the 2017–2018 Kharif and Rabi NDVI temporal and geographical variance in the research region. NDVI peaks in November, whereas Rabi season (November–April) peaks in February. The greatest NDVI score indicates crop peak growth in Kharif and Rabi seasons. Kharif season had a higher average NDVI than Rabi season, perhaps owing to factors that accelerated crop growth: Higher rainfall (south-west monsoon), increased photosynthesis due to longer sunny hours, and wider crop area in Kharif season.

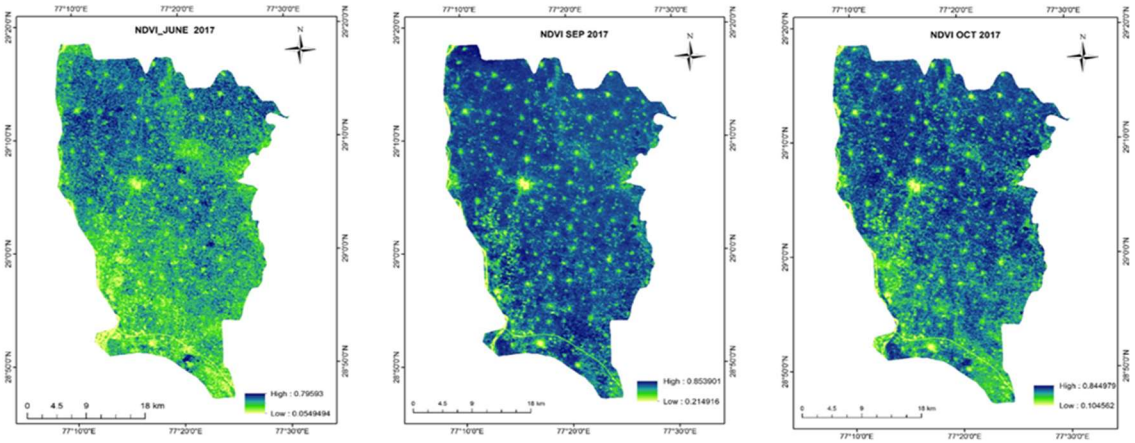

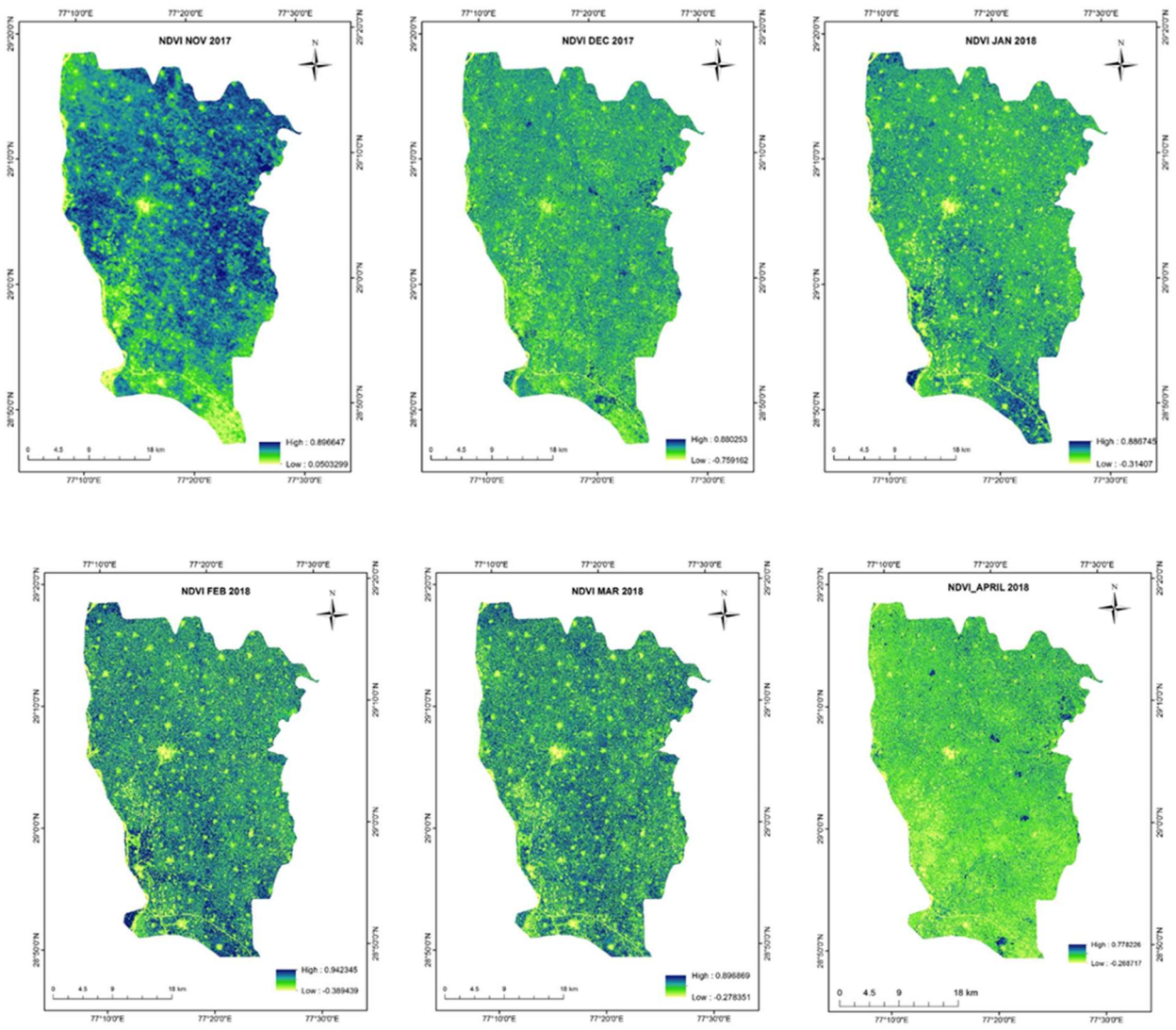


**Fig 4. Spatial distribution of NDVI for June 2017 to April 2018**

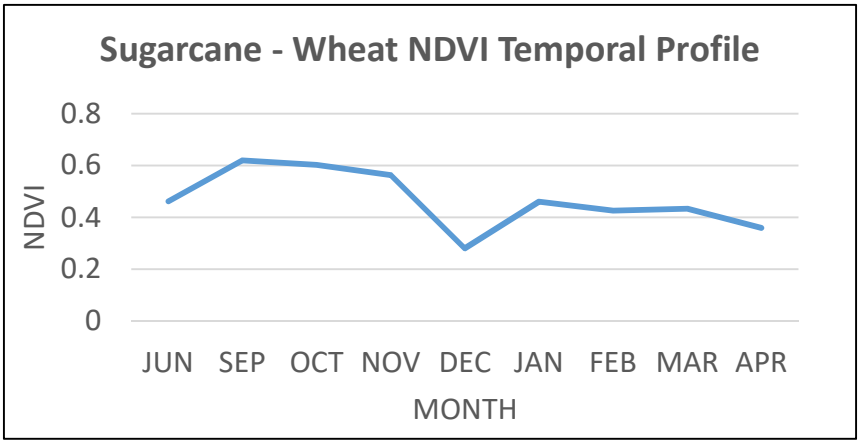


**Fig 5. Temporal variation in NDVI for sugarcane–wheat cropping system**

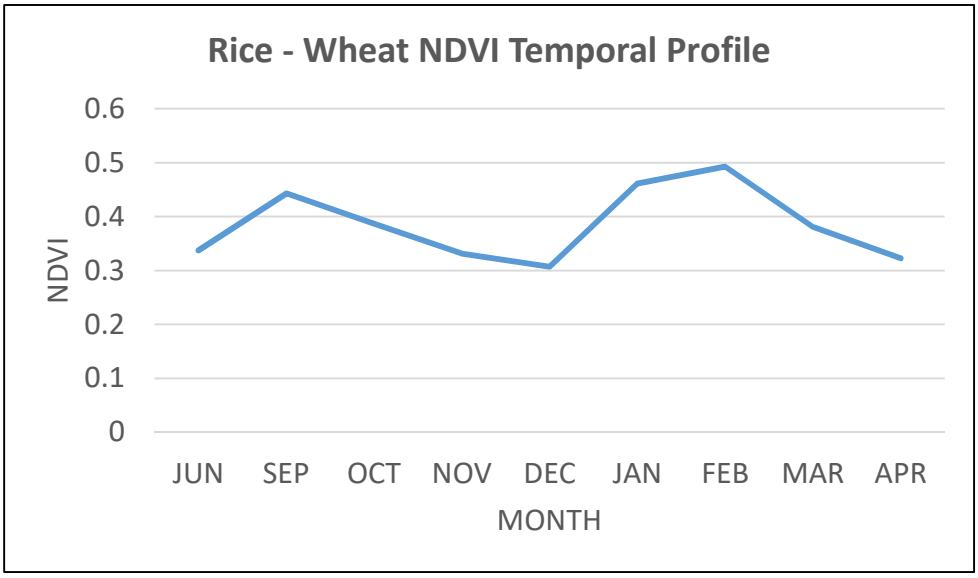


**Fig 6. Temporal variation in NDVI for rice–wheat cropping system**

The Normalized Difference Vegetation Index (NDVI) exhibited variability in relation to different crops and their phonological progression throughout the course of the growing season. The temporal fluctuations in NDVI for the sugarcane-wheat cropping system and the rice-wheat cropping system are shown in Figure 5 and 6, correspondingly. Figure 5.23 clearly demonstrates a decrease in NDVI values during December 2017. This decline corresponds to the development of wheat throughout the winter season after the harvest of sugarcane, as well as the early vegetative stage of sugarcane. The majority of the sugarcane crop was gathered in the month of December under the sugarcane-wheat agricultural system. Furthermore, a well-defined Normalized Difference Vegetation Index (NDVI) curve was found for the rice-wheat cropping system (refer to Figure 6). This curve clearly illustrates the trend of NDVI values while the rice and wheat crops undergo continuous phonological growth. These fundamental factors have effectively distinguished between the two systems. The observed NDVI patterns in this study exhibit similarities to the NDVI patterns reported by Kumari et al. (2013) in the context of sugarcane-wheat and rice-wheat cropping systems.

### 4.3 Basal Crop Coefficient

NDVI was used to derive the basal crop coefficient. The spatial representation of maps is below. Kcb and ETc fluctuated with crop and phenological development throughout the season, affecting crop water requirements. Fig.7 shows the temporal change of Kcb in Rice-Wheat and Sugarcane-Wheat cropping systems. Fig.7 show a fall in November and December 2017 owing to rice harvesting from Kharif season and a rise in Rabi season wheat transplanting. Rabi season adopts same profile. When temporal profile peaks, crop plant growth is maximum, hence water requirements are higher. The rice-wheat cropping system peaked in September and February with Kcb values of 1.2 and 1.23. In sugarcane-wheat cropping

system, Kcb temporal profile peaks in September and February with values of 1.24 and 1.03, although wheat peak value is low, perhaps because to mixed pixel combination with immature sugarcane plantings.

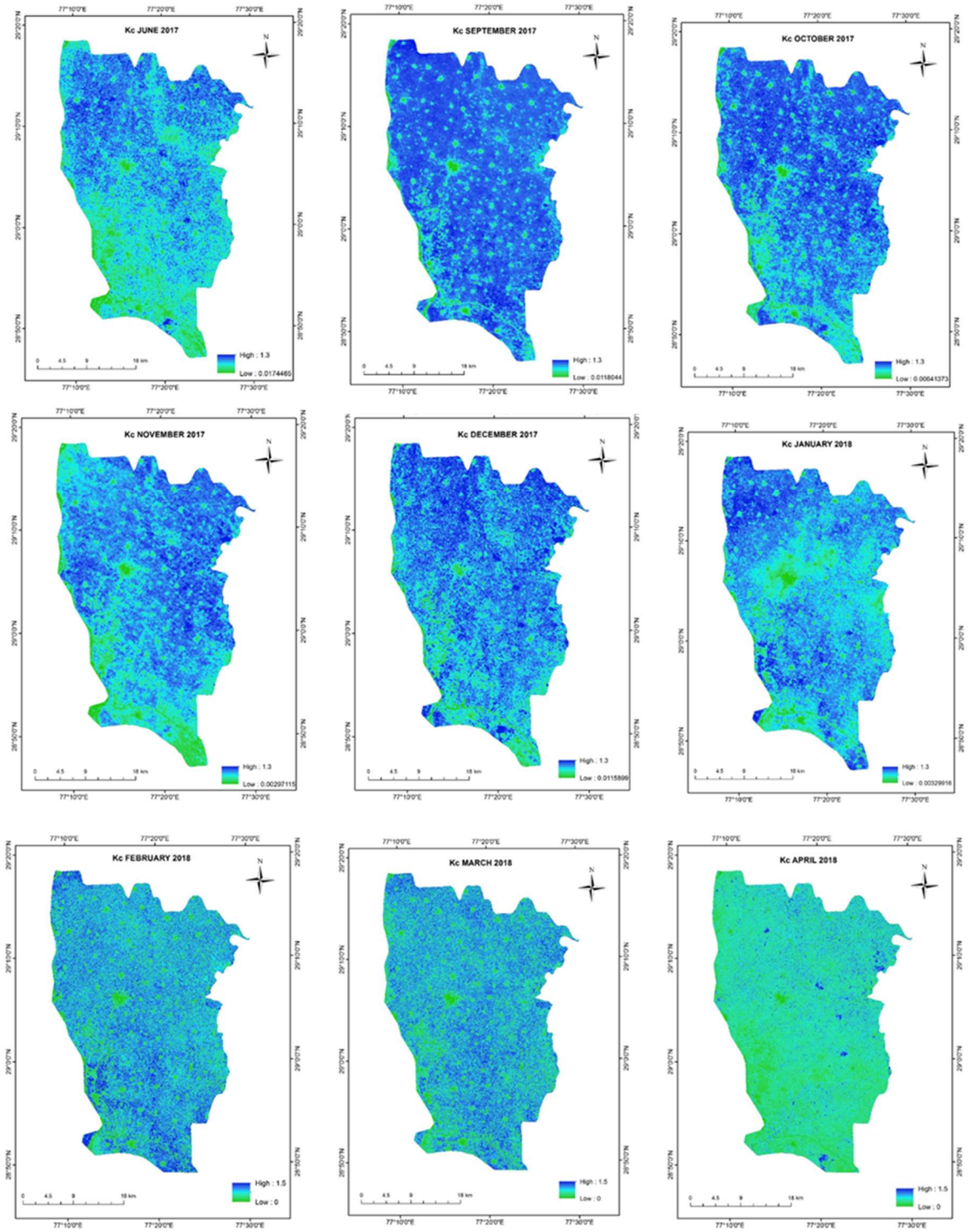


**Fig 7. Spatial distribution of Kcb for June 2017 to April 2018**

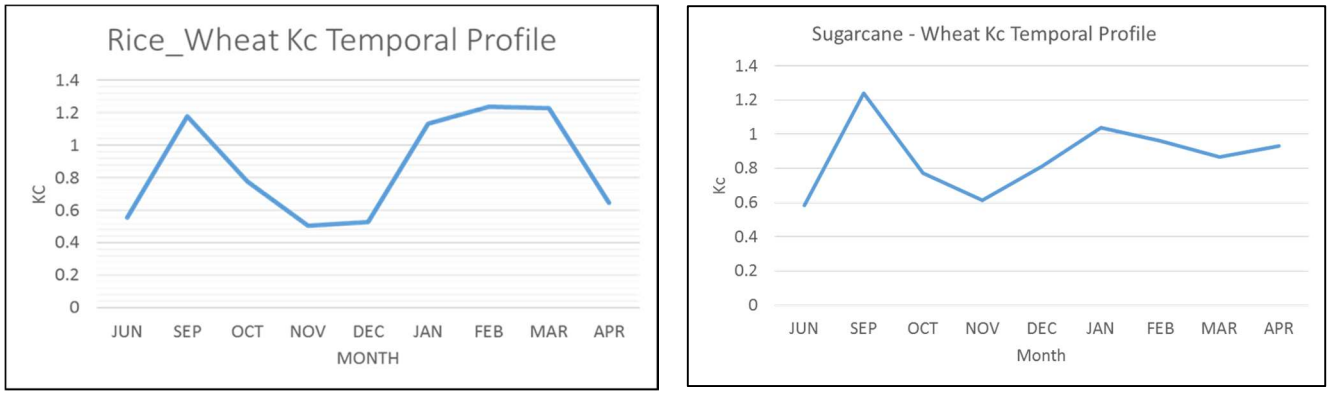


**Fig 8 Temporal variation in Kcb for rice–wheat & sugarcane–wheat cropping system**

### 4.4 Potential Evapotranpiration

The daily PET data downloaded from MOSDAC with a resolution of 5 km is resampled to 56 m resolution of AWiFS data. This is a daily average data product and the units of the PET data is in mm/day. The accuracy of the PET product is about 80-90% (INSAT-3D Manual, 2015). The temporal variation of daily PET as shown in figure 9. In Kharif and Rabi season the average value of PET in ranges between 4.41 to 5.91 mm/day and 3.30 to 5.42 mm/day

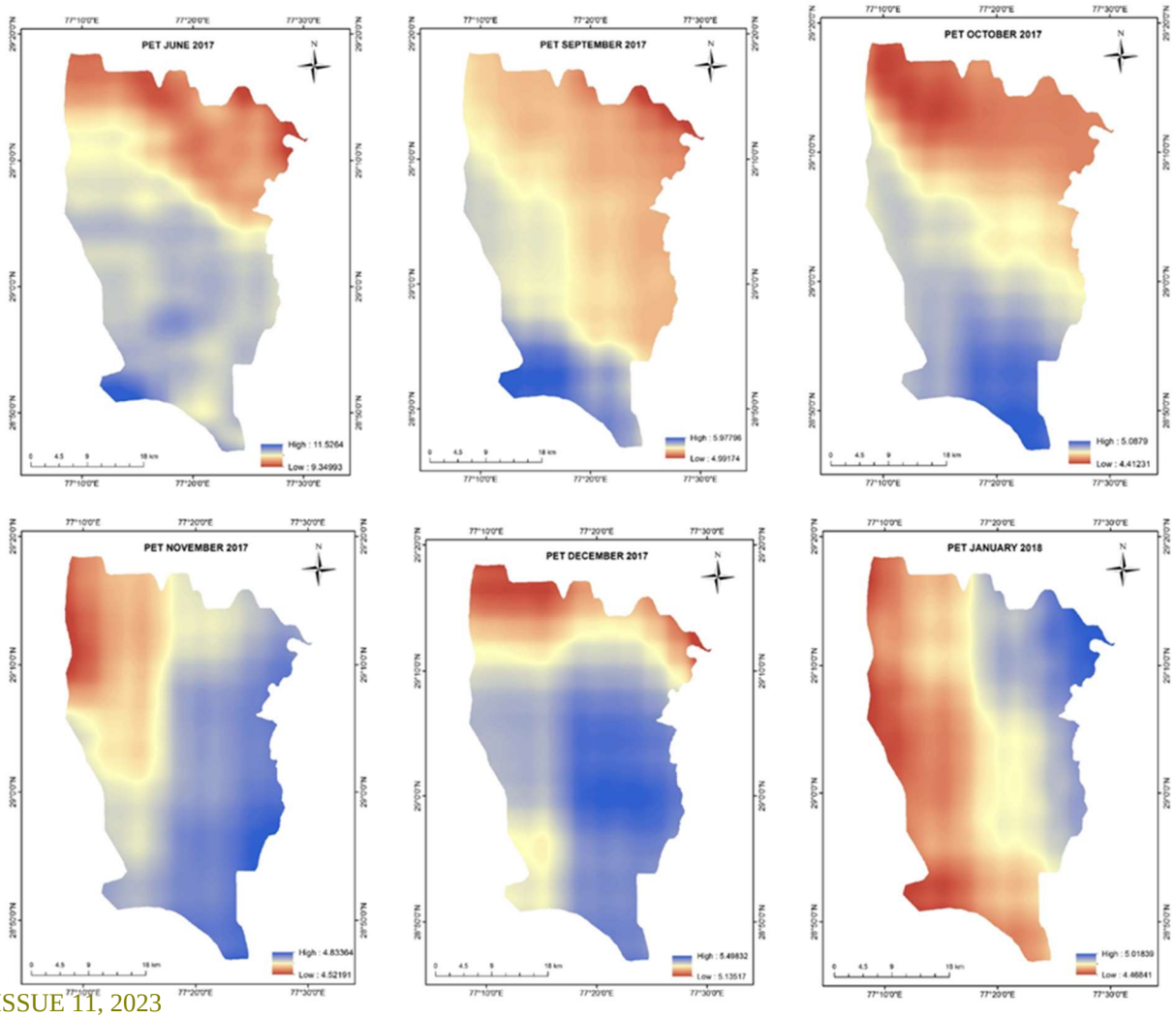

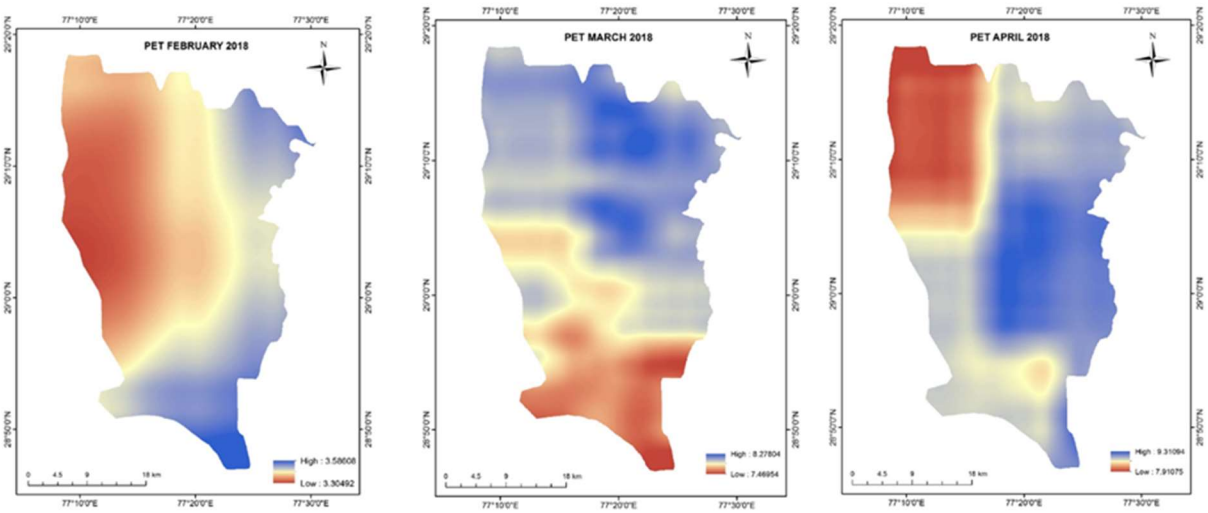


**Fig. 9 Spatial distribution of PET (mm/day) for June 2017 to April 2018**

### 4.5 Crop Evapotranspiration

The daily data from the PET (Potential Evapotranspiration) has been multiplied by the base crop coefficient (Kcb). The analysis of actual evapotranspiration (ET) based on the baseline crop coefficient and potential evapotranspiration (PET) reveals a marginal increase in ET during the month of November, followed by a fall in February. This may be attributed to the growth of sugarcane in November, with a significant portion being harvested by December. Lower readings are being recorded in February owing to the early vegetative development of wheat. The monthly photos exhibit a discernible pattern in the geographical distribution of monthly evapotranspiration. The evapotranspiration (ETc) exhibited a range of 3.09 to 6.87 mm day−1 throughout the period from June 2017 to April 2018. It is noteworthy that the mean ET value for sugarcane cultivation was determined to be 4.29 mm day−1. Sugarcane, a significant agricultural commodity in the nation, necessitates a substantial amount of water over its whole growth cycle, which typically spans 12 to 18 months. The specific duration may vary based on the agro-climatic areas, which range from sub-tropical to tropical. The crop's yearly water need in sub-tropical states like as Uttar Pradesh, Punjab, Haryana, and Bihar has been estimated to be 2000 mm (Shukla, S.K, 2017). The Food and Agriculture Organization (FAO) suggests that the range for this requirement falls between 1500-2500 mm. The estimated annual water demand for sugarcane in our research region is 2316.6 mm over a period of 18 months, and 1544.4 mm over a period of 12 months. The graphic shown below illustrates the spatial distribution of evapotranspiration (ET) and its temporal change.

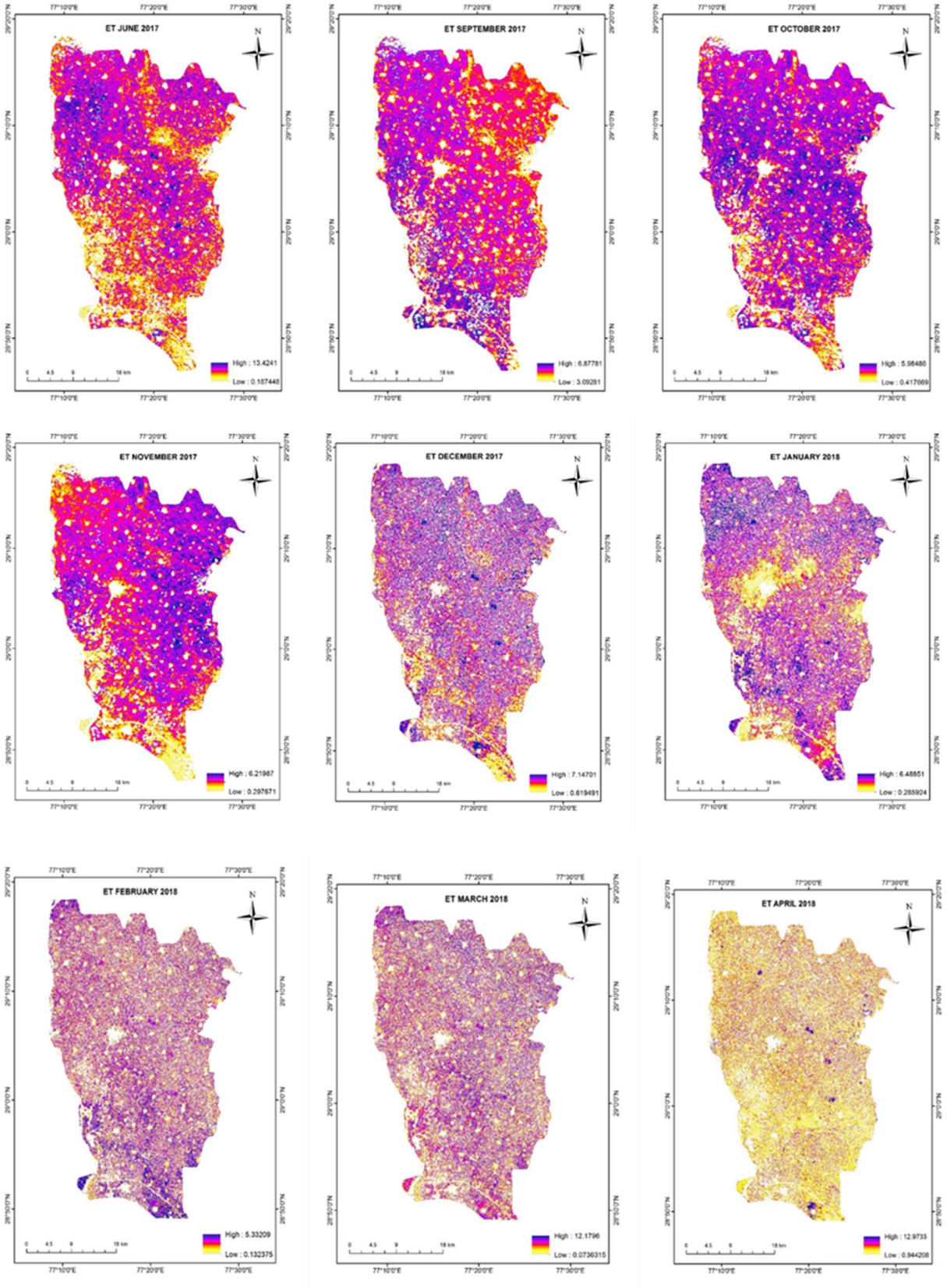


**Fig. 10 Spatial distribution of Daily ET (mm/day) for June 2017 to April 2018**

### 4.6 Land Surface Wetness Index (Lswi)

Land surface wetness index is a linear combination of NIR and SWIR bands. LSWI value ranges between -1 to +1 (Xiao et al., 2005).

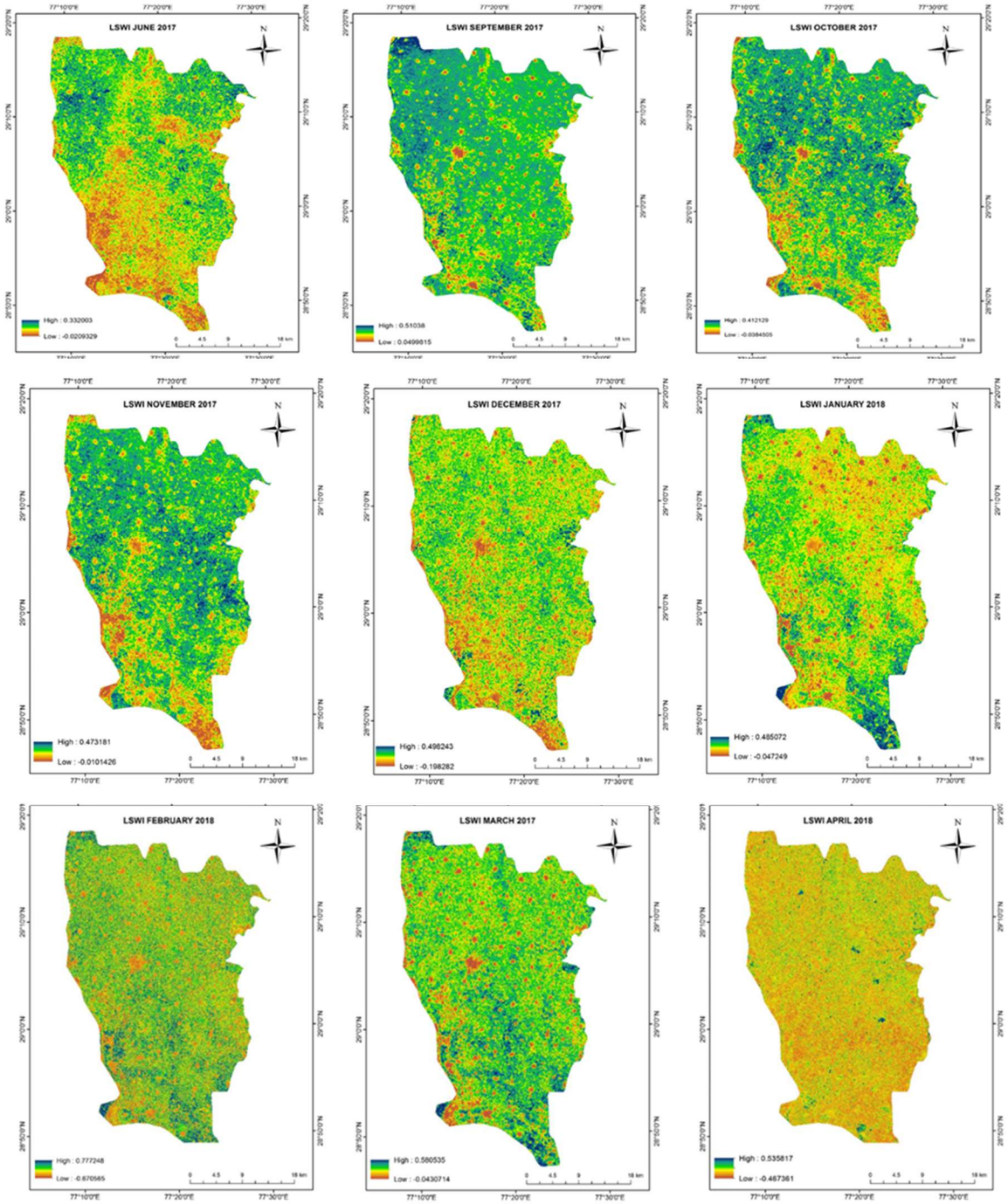


**Fig. 11 Spatial distribution of LSWI for November 2017 to April 2018**

### 4.7 Water Scalar Land Surface Wetness Index (Ws_Lswi)

The index is characterized by a numerical scale ranging from 0 to 1, with 0 denoting the absence of stress and 1 representing the presence of severe stress. The time distribution of water scalar may be noticed in Figure 5.71. Based on the findings from the period spanning June 2017 to January 2018, the observed trend may be attributed to the successive cultivation of kharif crops followed by rabi crops, leading to increased strain on the agricultural system. Subsequently, from February to April, the recorded values indicate a decline, which can be attributed to the commencement of crop harvesting during this period. In the month of June, a stress level of 0.56 was detected. However, in the subsequent months of September and October, the stress level exhibited a declining trend due to the increased vegetative development of sugarcane and rice crops. In November, there was a modest rise in the stress level, and by December, the value reached 0.50. This increase in stress may be attributed to the harvesting activities of rice and the presence of older sugarcane farms. The water scaler values show a decline subsequent to December, indicating a decrease in water stress. This trend aligns with the development of wheat crops occurring in January, February, and March. However, in April, a greater level of stress is noticed, as indicated by a value of 0.69, which may be attributed to the harvesting of wheat during this period.

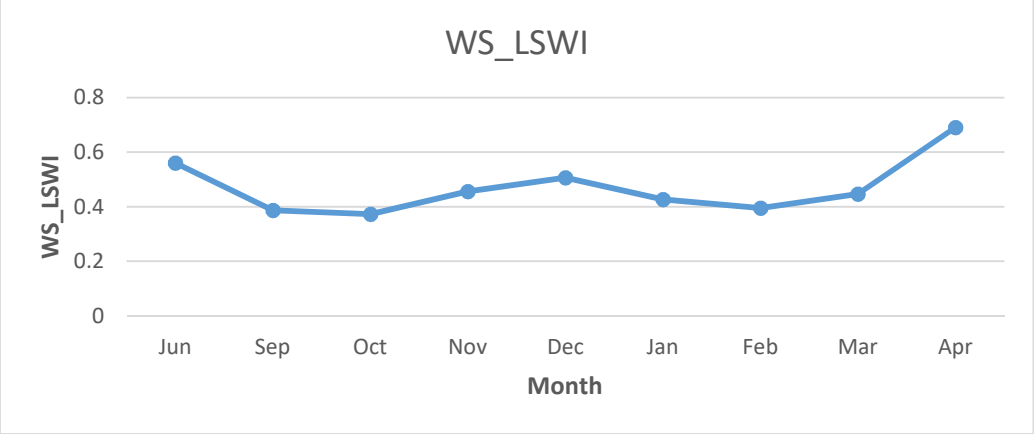


**Fig. 12 Temporal variation in WS_LSWI**

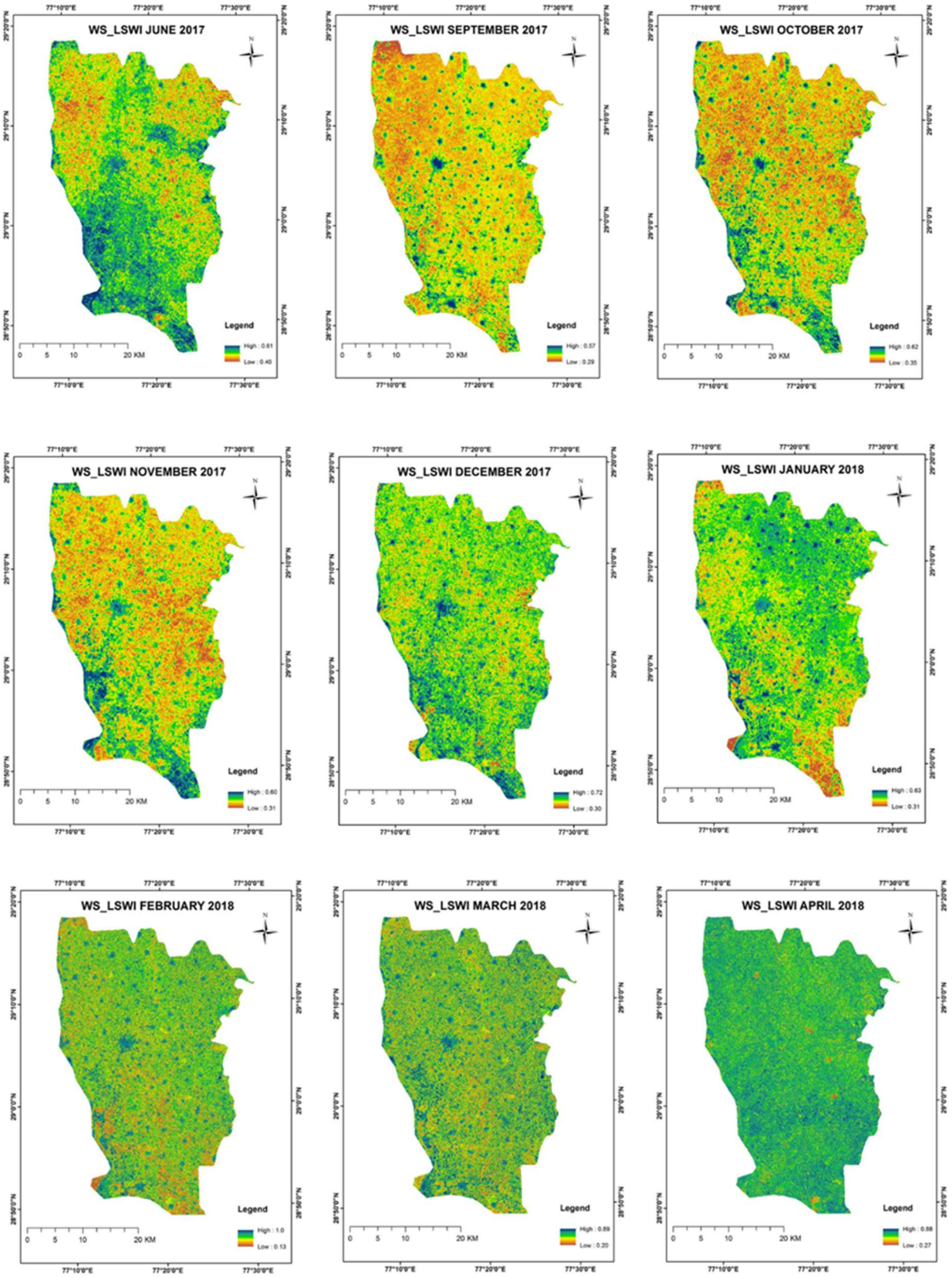


**Fig. 13 Spatial distribution of WS_LSWI for June 2017 to April 2018**

## CONCLUSIONS

The current work used a remote sensing-based technique to estimate crop evapotranspiration (ETc) from Bagpath, located in Western Uttar Pradesh. A rule-based classification using the Normalized Difference Vegetation Index (NDVI) was conducted to classify Kharif and Rabi Seasons. This included establishing thresholds for various classes within the research region. The resulting classification achieved an overall accuracy of 86.86% for Kharif crops and 79.72% for Rabi crops. The kappa coefficients for Kharif and Rabi crops were determined to be 0.81 and 0.712, respectively. The assessment of the NDVI profile effectively covers the growth season of the sugarcane-wheat and rice-wheat cropping system, allowing precise crop mapping within the designated research region. During the Kharif and Rabi seasons, the mean potential evapotranspiration (PET) varies from 4.41 to 5.91 mm/day and 3.30 to 5.42 mm/day, respectively. In the rice-wheat cropping system, a notable surge was seen between the months of September and February, with corresponding Kcb values of 1.2 and 1.23, respectively. The temporal profile of Kcb in the sugarcane-wheat cropping system exhibits peaks in the months of September and February, with corresponding values of 1.24 and 1.03, respectively. However, it is seen that the peak value of wheat is relatively lower, which might perhaps be attributed to the presence of mixed pixels resulting from the mixture of young sugarcane plants. The evapotranspiration (ETc) exhibited a range of 3.09 to 6.87 mm day−1 throughout the period spanning from June 2017 to April 2018. It is worth noting that the average ET value for sugarcane cultivation was determined to be 4.29 mm day−1. The estimated yearly water demand for sugarcane in our research region is 2316.6 mm over a period of 18 months and 1544.4 mm over a period of 12 months. The WS_LSWI data was collected between June 2017 and January 2018. In the month of June, a stress level of 0.56 was recorded. However, in the subsequent months of September and October, the stress level exhibited a downward trend due to the significant rise in vegetative development of sugarcane and rice crops. In November, there was a modest increase in stress levels, which may be attributed to certain factors. Finally, by December, the stress level reached a value of 0.50, likely due to the harvesting activities of rice and the presence of older sugarcane farms. The water scaler readings show a decline subsequent to the month of December, indicating a decrease in water stress. This decline coincides with the growing period of the wheat crop, which occurs mostly in the months of January, February, and March. However, in April, a greater level of water stress is detected, with a recorded value of 0.69. This increase in stress may be attributed to the harvesting of the wheat crop during this period.

## REFERENCES

Aerosol Optical Depth, Water Vapor and Ozone data from https://giovanni.gsfc.nasa.gov/giovanni/

Atmospheric Correction Model for Resourcesat-2 AWiFS data (SACRS2) and INSAT_3D_PET_Daily data from June 2017 to April 2018 from MOSDAC (Meteorological and Oceanographic Satellite Data Archival Centre).

Azzali, S.; Menenti, M. Mapping isogrowth zones on continental scale using temporal Fourier analysis of AVHRR-NDVI data. *Int. J. Appl. Earth Obs. Geoinform.* **1999**, *1*, 9–20.

Chavez, P.S., 1996. Image-based atmospheric corrections-revisited and improved. Photogramm. Eng. Remote Sens. 62, 1025–1035.

Claudio, H.C., Cheng, Y., Fuentes, D.A., Gamon, J.A., Luo, H., Oechel, W., Qiu, H.-L., Rahman, A.F., Sims, D.A., 2006. Monitoring drought effects on vegetation water content and fluxes in chaparral with the 970 nm water band index. Remote Sens. Environ. 103, 304–311.

Clawson, K.L., Blad, B.L., 1982. Infrared thermometry for scheduling irrigation of corn. Agron. J. 74, 311–316.

Cohen, W.B., 1991. Response of vegetation indices to changes in three measures of leaf water stress.

DeFries, R., Hansen, M., Townshend, J., 1995. Global discrimination of land cover types from metrics derived from AVHRR Pathfinder data. Remote Sens. Environ. 54, 209–222.

Dixon, Henry H., "Transpiration and the ascent of sap in plants", (London: Macmillan, 1914).

FAO Crop Water Needs, http://www.fao.org/docrep/s2022e/s2022e02.htm

FAO. 2008. Expert meeting on Climate change, water and food security. 26–28 February 2008. Contribution to the High Level Conference on World Food Security and the Challenge of Climate Change and Bio-energy on Water and Climate Change.

FAO. 2011a. Climate change, water and food security. Prepared by H. Turral, J. Burke and J.-M. Faurès. FAO Water Reports, no. 36.

Gao, B.-C., 1996. NDWI—a normalized difference water index for remote sensing of vegetation liquid water from space. Remote Sens. Environ. 58, 257–266.

Ghulam, A., Li, Z.-L., Qin, Q., Yimit, H., Wang, J., 2008. Estimating crop water stress with ETM+ NIR and SWIR data. Agric. For. Meteorol. 148, 1679–1695.

Hardisky, M.A., Klemas, V., Smart, M., 1983. The influence of soil salinity, growth form, and leaf moisture on the spectral radiance of. Spartina Alterniflora 77–83.

Hooda, R.S., DYE, D., 1995. Identification and mapping irrigated vegetation using NDVI-Climatological modeling: In: Proceeding of ACRS. Thiland.

Hunt Jr, R., Rock, B.N., Nobel, P.S., 1987. Measurement of leaf relative water content by infrared reflectance. Remote Sens. Environ. 22, 429–435.

Idso, S.B., 1982. Non-water-stressed baselines: a key to measuring and interpreting plant water stress. Agric. Meteorol. 27, 59–70.

Idso, S.B., Jackson, R.D., Reginato, R.J., 1977. Remote sensing for agricultural water management and crop yield prediction. Agric. Water Manag. 1, 299–310.

IPCC. 2008. Climate Change and Water. Edited by B.C. Bates, Z.W. Kundzewicz, S. Wu and J.P. Palutikof. IPCC Technical Paper VI. IPCC Secretariat, Geneva. 210 p.

Jackson, R.D., Idso, S.B., Reginato, R.J., Pinter, P.J., 1981. Canopy temperature as a crop water stress indicator. Water Resour. Res. 17, 1133–1138.

Jiang, L., Islam, S., 2001. Estimation of surface evaporation map over southern Great Plains using remote sensing data. Water Resour. Res. 37, 329–340.

Kumari M, Patel NR, Khayruloevich PY. 2013. Estimation of crop water requirement in rice-wheat system from multitemporal AWIFS satellite data. Int J Geomatics Geosci. 4(1):61–74.

Lichtenthaler, H.K. Chlorophylls and carotenoids: pigments of photosynthetic biomembranes. In: PACKER, L.; DOUCE, R. (Ed.) Methods in enzimology. London: Academic Press, 1987. v. 148, p. 350-381.

Lillesand TM, Kiefer RW. 1999. Remote sensing and image interpretation. New York (NY): Wiley. Lo SCD, Mougin E, Gastellu-Etchegorry JP. 1993. Relating the global vegetation index to net primary productivity and actual evapotranspiration over Africa. Int J Remote Sens. 14:1517–1546.

López López, R., Arteaga Ramírez, R., Vázquez Peña, M.A., López Cruz, I., Sánchez Cohen, I., 2009. Índice de estrés hídrico como un indicador del momento de riego en cultivos agrícolas. Agric. Téc. En México 35, 97–111.

Lu, D., Mausel, P., Brondizio, E., & Moran, E. (2002), Assessment of atmospheric correction methods for Landsat TM data applicable to Amazon basin LBA research. International Journal of Remote Sensing, 23(13), 2651-2671.

Moran, M.S., Clarke, T.R., Inoue, Y., Vidal, A., 1994. Estimating crop water deficit using the relation between surface-air temperature and spectral vegetation index. Remote Sens. Environ. 49, 246–263.

Müller NJC (1874) Beziehungen zwischen Assimilation, Absorption und Fluoreszenz im Chlorophyll des lebenden Blattes. Jahrbuch wiss Botanik 9, 42–49.

Navalgund, R.R., Parihar Ajai, J.S., Nageshwara Rao, P.P., 1991b. Crop inventory using remotely sensed data. Curr. Sci. 61, 162–171.

Nitika Dangwal, N.R. Patel, Mamta Kumari & S.K. Saha (2016) Monitoring of water stress in wheat using multispectral indices derived from Landsat-TM, Geocarto International, 31:6, 682-693.

Pandya M. R., Pathak V. N., Shah D. B., Trivedi H. J. Chipade R. A., Singh R.P., Kirankumar A. S. (2015), Development of a scheme for atmospheric correction of Resourcesat-2 AWiFS data. International Journal of Applied Earth Observation and Geoinformation 40, 65-73.

Parodi, G. (2005), Introduction to atmospheric correction of visible and thermal imagery: Basic text, Enschede, pp. 58.

Patel NR, Rakhesh D, Mohammed AJ. 2006. Mapping of regional evapotranspiration in wheat using Terra/MODIS

Patel, N.R., Mehta, A.N., Shekh, A.M., 2001. Canopy temperature and water stress quantificaiton in rainfed pigeonpea (< i> Cajanus cajan</i>(L.) Millsp.). Agric. For. Meteorol. 109, 223–232.

Phansalkar, Sanjiv; Verma, Shilp. 2005. Mainstreaming the margins: water-centric livelihood strategies for revitalizing tribal agriculture in Central India. New Delhi, India: Angus and Grapher. xi, 212p.

Porporato, A., Laio, F., Ridolfi, L. & Rodriguez-Iturbe, I. (2001) Plants in water-controlled ecosystems: active role in hydrological processes and response to water stress. III. Vegetation water stress. Adv. Wat. Resour. 24(7), 725-744.

Price, J.C., 1987. Calibration of satellite radiometers and the comparison of vegetation indices. Remote Sens. Environ. 21, 15–27.

Reynolds, C.A., Yitayew, M., Slack, D.C., Hutchinson, C.F., Huete, A., Petersen, M.S., 2000. Estimating crop yields and production by integrating the FAO Crop Specific Water Balance model with real-time satellite data and ground-based ancillary data. Int. J. Remote Sens. 21, 3487–3508.

Ripple, W.J., 1986. Spectral reflectance relationships to leaf water stress.

Sabins Jr, F.F., n.d. Remote Sensing, Principles and Interpretation. 1978. San Francisco, WH Freeman & Co.satellite data. Hydrol Sci J. 51(2):325–335.

ŞENCAN, S., 2004. DECISION TREE CLASSIFICATION OF MULTI-TEMPORAL IMAGES FOR FIELD-BASED CROP MAPPING. MIDDLE EAST TECHNICAL UNIVERSITY.

Shukla, S.K.; Sharma, Lalan; Awasthi, S.K.; Pathak,A.D.(2017), Sugarcane in India: Package of Practices for Different Agro-climatic Zones, Page No. 1-64

Slater, P.N., 1980. Remote sensing: optics and optical systems. Read. Mass Addison-Wesley Publ. CoRemote Sens. No 1 1980 593 P 1.

Tucker, C.J., 1980. Remote sensing of leaf water content in the near infrared. Remote Sens. Environ. 10, 23–32.

Usman, M., Ahmad, A., Ahmad, S., Arshad, M., Khaliq, T., Wajid, A., Hussain, K., Nasim, W., Chattha, T.M., Trethowan, R., 2009. Development and application of crop water stress index for scheduling irrigation in cotton (Gossypium hirsutum L.) under semiarid environment. J. Food Agric. Environ. 7, 386–391.

Vermote, E.F., El Saleous, N.Z., Justice, C.O., 2002. Atmospheric correction of MODIS data in the visible to middle infrared: first results. Remote Sens. Environ. 83, 97–111.

Xiao, X., Zhang, Q., Braswell, B., Urbanski, S., Boles, S., Wofsy, S., Moore III, B., Ojima, D., 2004. Modeling gross primary production of temperate deciduous broadleaf forest using satellite images and climate data. Remote Sens. Environ. 91, 256–270.

Zarco-Tejada, P. J., Miller, J. R., Mohammed, G. H., and No land, T. L. (2000), Chlorophyll fluorescence effects on vegetation apparent reflectance: I. Leaf-level measurements and model simulation. Remote Sens. Environ. (this issue).